Phys. Status Solidi B **247**, Nos. 11–12, 2660–2663 (2010) / **DOI** 10.1002/pssb.201000120

physica status solidi b
www.pss-b.com
basic solid state physics

Analysis of carbon nanotube chiralities obtained from a bimetallic Co-Mo catalyst

Martin Fouquet*[,1], Stephan Hofmann[1], Christian Thomsen[2], and John Robertson[1]

[1] Department of Engineering, University of Cambridge, Cambridge CB3 0FA, UK
[2] Institut für Festkörperphysik, Technische Universität Berlin, 10623 Berlin, Germany

Received 21 April 2010, revised 17 May 2010, accepted 25 May 2010
Published online 23 August 2010

Keywords carbon nanotubes, chiral map, growth, Raman, SWNT

* Corresponding author: e-mail mf398@cam.ac.uk, Phone: +44-(0)1223-748377, Fax: +44-(0)1223-748348

All growth methods for single-walled carbon nanotubes (SWNTs) usually result in a wide distribution of chiral indices (*n*,*m*). Bimetallic catalysts can narrow this distribution [1,2]. Here we grow SWNTs by a Co-Mo catalyst and measure the different chiral distributions for an array of growth parameters. A CoMo-acetate solution as described by Miyauchi et al. [1] was used to prepare the catalyst. With chiral maps we find that the absolute diameter range for the SWNT is about 0.7–1.7 nm for all samples. Hereby metallic and semiconducting tubes favour different diameters and thus divide the full range in two intervals. Histogramms made for the chiral angle distribution of the assigned SWNT suggest that semiconducting tubes favour a chiral angle of 20°–25°.

1 Introduction Single-walled carbon nanotubes (SWNT) come in many different configurations (*i.e.* diameter, electronic properties, *etc.*). They can be semiconducting or metallic depending on the arrangement of carbon hexagons forming the nanotube. This arrangement of hexagons is described by the chiral indices (*n*,*m*). Each SWNT has a unique chiral index which can be used to derive the structural and electronic properties [3]. This means the band gap can be tailored to a desired value by selecting the matching tube, or metallic tubes can be used as very small interconnects replacing *e.g.* copper. Thus, SWNTs are extremely promising for nanoscale applications. However, all the advantages come with one major disadvantage: wide chiral distributions during the growth process. There are ways of sorting the growth product in terms of diameter, metallic or semiconducting behaviour or even chiral indices [4–6], but intensive postgrowth processing is unwanted or even impossible for most large scale applications. Ideally the individual semiconducting SWNT with the desired band gap or the small bundle of small diameter metallic SWNT is directly and reliably grown where it is needed. Therefore, the distribution of nanotubes produced by a growth process needs to be very narrow and ideally only tubes with one chiral index will be grown. A first step is to control the catalyst particle size [7, 8] since particle size can be directly related to the SWNT diameter [9, 10]. This will already significantly limit the number of different chiral indices. But for a small diameter range there are still many chiral indices. The challenge to limit those remains. The CoMoCat process [2, 11] has shown to be a possible solution for that by using high pressure (5 bar) and CO as carbon precursor. Even highly dense vertical aligned SWNTs were grown by using this bimetallic catalyst for high pressure CO [11] or low pressure (mbar range) ethanol [12, 13]. Cobalt and molybdenum in this case or in general the use of a bimetallic catalyst, can produce a narrow diameter and chiral distribution [1, 2, 14, 15] and the SWNT tend to be mainly semiconducting. This may limit the use as interconnects in integrated circuits as was pointed out by Robertson et al. [16]. Thus so far experimental conditions like high temperature or pressure may limit the direct production of a device based on single chirality SWNT. Investigation of the chiral distribution with respect to certain growth and pretreatment conditions is thus needed if not mandatory.

Here we present growth of SWNT by a CoMo catalyst for a variation of growth parameters followed by a multiwavelength Raman analysis. We find a rather large diameter range for the SWNT but the large range divides into two smaller intervals with mainly metallic or semiconducting tubes.

2 Experimental details and discussion The SWNT growth was carried out in a cold wall low pressure chemical vapour deposition (lpCVD) system in which the temperature was controlled by an electrical operated boron-

nitride heating plate and measured by a thermocouple attached to the heater, as well as by pyrometer measurements on the sample itself. H_2 or NH_3 were used for pretreatment of the catalyst and C_2H_2 or EtOH was used as the carbon precursor. All growth products were investigated with a scanning electron microscope (SEM) after growth and in the case of finding networks of carbon nanotubes (CNTs) Raman measurements were carried out. Raman measurements were performed on a confocal micro-Raman setup (Dilor XY) in backscattering geometry. Eight laserlines of an ArKr-laser ranging from 465 to 647 nm were used for excitation. The spectra were recorded with a charge coupled device (CCD) cooled by liquid nitrogen and neon lines were used for calibration.

Preparation of the catalyst by dipcoating a cobalt acetate molybdenum acetate solution on a Si-waferpiece was done by Miyauchi et al. [1]. The catalyst was calcinated at 400 °C in air at atmospheric pressure for 10 min. Growth was carried out by heating in the pretreatment gas (H_2 or NH_3) for 5 min to the growth temperature (450–750 °C). After removal of the pretreatment gas the carbon precursor (C_2H_2 or EtOH) was introduced.

The growth time was kept at 15 min after which the precursor was removed and the system was left to cool in vacuum. The pressure was kept the same for both pretreatment and growth and varied from 1.3×10^{-3} to 5 mbar.

Each growth product was investigated with SEM and it was found that a temperature of 625–750 °C was needed to grow any CNTs. Figure 1 shows two exemplary growth results. If CNTs grew it resulted in an entangled network of SWNTs with very minor differences in yield for different growth conditions. In general the use of C_2H_2 produced SWNT for the complete pressure range whereas EtOH only showed growth for a pressure of around 0.5 and 5 mbar and no growth at all at 10^{-3} mbar. Although EtOH was more sensitive to the pressure, the overall quality of the SWNT was better when compared to C_2H_2. This behaviour is shown in Fig. 2 by plotting the ratio G/D between the intensities of the G-mode and the D-mode as function of the growth pressure at an excitation wavelength of 476 nm. The G/D ratio is not good when compared to other results (*i.e.* Ref. [12]). But since the SWNT in our case form an entangled network which is not covering the substrate completely as shown in Fig. 1, a strong contribution from amorphous carbon from the SWNT-free areas is believed. This and the strong and sharp peaks for the radial breathing mode (RBM) as shown in Fig. 3a suggest that the bad G/D-ratio may not refer to bad quality SWNT. Raman spectroscopy was done for each SWNT sample and eight different excitation energies. The RBM was measured. Each peak encountered in the spectra was fitted with a lorentzian and the peak position ω_{RBM} was used to derive the tube diameter d with the inverse relationship from Eq. (1) [3]:

$$\omega_{RBM} = \frac{A}{d} + B. \quad (1)$$

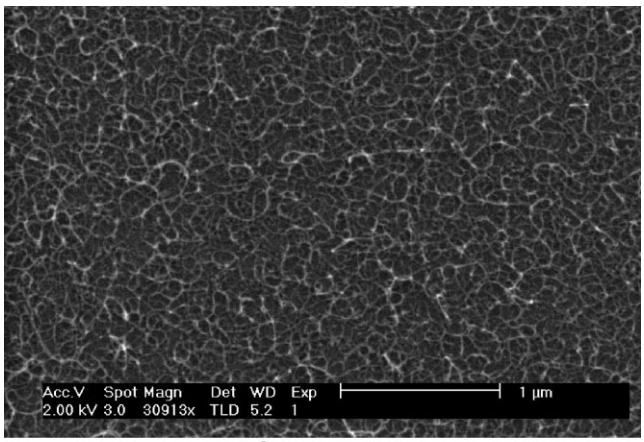

a) NH_3/C2H2 at $1.3x10^{-3}$ mbar, 660 °C

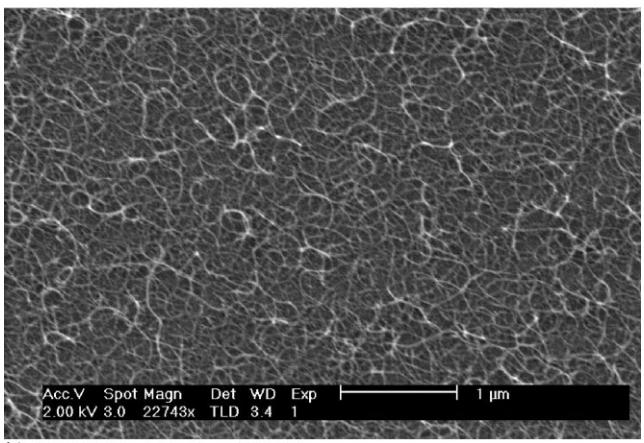

b) H_2/EtOH at 5 mbar, 740 °C

Figure 1 Two example SEM images for the SWNT growth. The tubes were always grown as entangled network.

The values for the constants A and B were taken from Telg et al. [17]. As an example of the Raman spectra the waterfall diagram in Fig. 3a is shown. The diagram shows Raman spectra with several RBM peaks for all eight

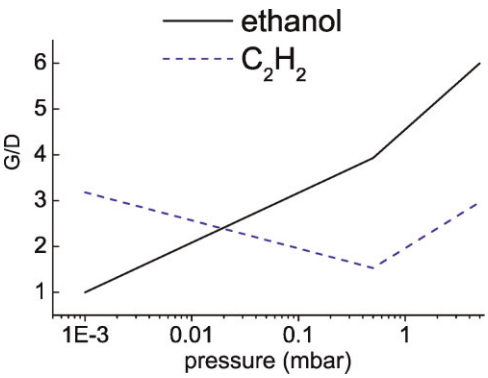

Figure 2 (online colour at: www.pss-b.com) The ratio of the G-mode divided by the D-mode intensities is shown as function of the growth pressure for ethanol (black, solid line) and C_2H_2 (blue, dashed line). The ratios were taken for an excitation wavelength of 476 nm.

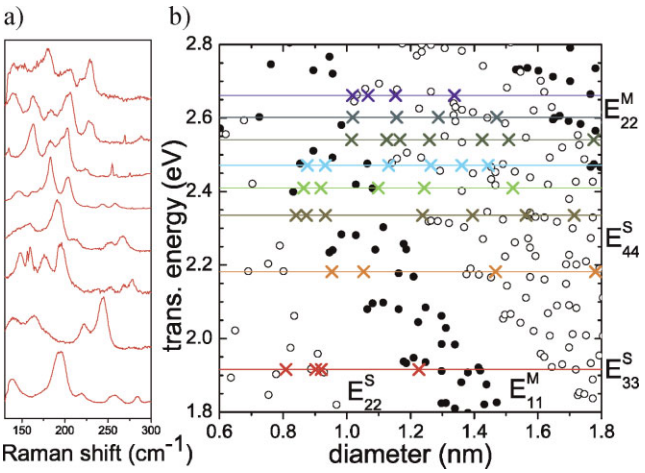

Figure 3 (online colour at: www.pss-b.com) Raman spectra (a) and Kataura plot (b) for the sample shown in Fig. 1b. The crosses in the Kataura plot mark the positions for the SWNT encountered in the Raman spectra for the corresponding wavelength.

excitation energies. The SWNT for these spectra are the same as in Fig. 1b. The excitation energy E_{laser} and the diameter d provide the two necessary parameters to assign a peak in the Raman spectrum to a SWNT's chiral index (n,m) in the Kataura plot. For the assignment a Kataura plot based on a nonorthogonal tight-binding model, with an empirical 0.3 eV blueshift, is used [18] and shown in Fig. 3b. As E_{laser} is not necessarily matching the transition energy E_{ii}, sometimes a large offset can be expected. But as the excitation energies E_{laser} are close enough for mostly two E_{laser} values to be included in the resonance window of the same tube a reasonable assignment is possible. Nonetheless it has to be pointed out that the limited set of excitation energies may miss some of the possible SWNT. This may cause some artificial preferential diameter distributions for SWNTs. Considering our excitation energies in the Kataura plot in Fig. 3b we are confident to find metallic SWNT for a diameter range of 0.7–1.5 nm and semiconducting tubes for diameters ranging from 0.6 to 1.8 nm (excluding a few CNT around 1.0–1.2 nm). The SWNT for the remaining diameters have a transition energy to far away from the laser energies used. The assignment for all SWNT in a single growth process can be summarized in a chiral map. An example of these chiral maps is shown in Fig. 4 for the same SWNT shown in the SEM images in Fig. 1. In general the SWNT of all growth processes show an absolute diameter range of 0.7–1.7 nm. Although this range is quite large the majority of tubes are found in two smaller intervals. As an average over all chiral maps it is seen that the metallic tubes strongly favour an average diameter of 0.8–1.0 nm and the semiconducting tubes are mostly found in the interval from 1.1 to 1.3 nm. Many of the semiconducting tubes show a chiral angle of 20°–25° whereas the metallic SWNT are evenly distributed for chiral angles between 0° and 30°. The chiral angle distribution is shown in Fig. 5. The reason for different preferential diameters or chiral angles is most likely the catalyst composition. Chiang and Sankaran [19] found that the ratio between two growth-active metals (Fe and Ni in their case) can influence the chiral distribution. Although only Co is active in the growth conditions we used, a similar effect is believed. For a pretreatment in NH_3, although the absolute diameter range for the SWNT did not change, the number of different chiral indices increases. This may either be caused by having more particles in the required metallic state [20] or the influence of the gas composition on the catalyst [21].

Finally it has to be pointed out that the chiral maps only yield information about the existence of at least one SWNT with a given chiral index (n,m). The amount of SWNT with the same (n,m) as a percentage of the whole sample could not be estimated by the data acquired so far.

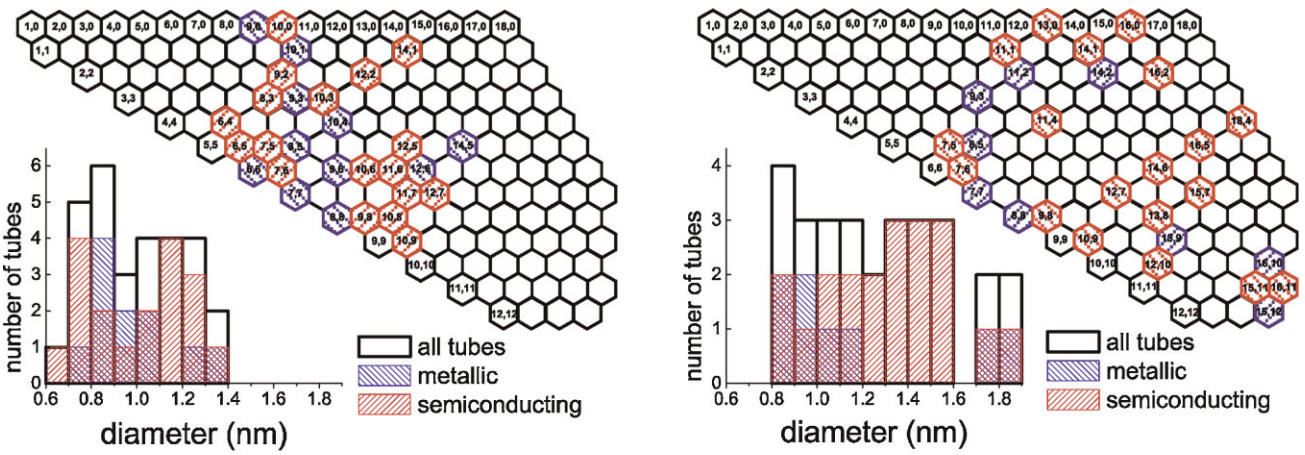

Figure 4 (online colour at: www.pss-b.com) Chiral maps and diameter distributions for the same two samples shown in Fig. 1. Metallic tubes are marked in blue (downward diagonal) and semiconducting tubes in red (upward diagonal).

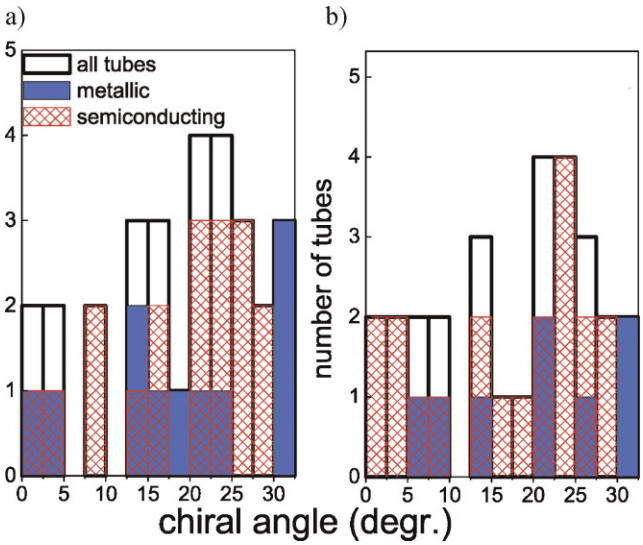

Figure 5 (online colour at: www.pss-b.com) Chiral angle distribution for the two examples. Metallic tubes are marked in blue (downward diagonal) and semiconducting tubes in red (upward diagonal).

3 Conclusion In summary growth of SWNT on CoMo catalysts followed by multiwavelength Raman spectroscopy on the RBM for chiral maps was presented. The growth was done for two different pretreatment gases, H_2 or NH_3, and two carbon precursors, C_2H_2 or EtOH, for a pressure range of 1.3×10^{-3}–5 mbar and a temperature range of 450–750 °C. It was found that a temperature of at least 625 °C was needed to grow nanotubes and a higher pressure for EtOH-based growth in comparison to C_2H_2-based growth. The chiral maps have shown that the absolute SWNT diameter range of 0.7–1.7 nm divides in two intervals one with mainly metallic tubes (0.8–1.0 nm) and the other with mainly semiconducting (1.1–1.3 nm) tubes. The semiconducting tubes favoured a chiral angle around 20°–25° and metallic tubes did not show any angle preference. Diameter and chiral angle preferences may be caused by catalyst composition. NH_3 as pretreatment gas results in a wider chiral distribution but the same diameter distribution of the SWNT. This was attributed to more catalyst particles in the metallic state or the difference in pretreatment gas compositions. Although the abundance of each chiral index (n,m). could not be estimated future work should yield results for this.

Acknowledgements The group of Prof. Maruyama et al. is acknowledged for preparation of the CoMo catalyst. Funding from the EC project technotubes is acknowledged.

References

[1] Y. H. Miyauchi, S. H. Chiashi, Y. Murakami, Y. Hayashida, and S. Maruyama, Chem. Phys. Lett. **387**, 198 (2004).
[2] S. M. Bachilo, L. Balzano, J. E. Herrera, F. Pompeo, D. E. Resasco, and R. B. Weisman, J. Am. Chem. Soc. **125**, 11186 (2003).
[3] S. Reich, C. Thomsen, and J. Maultzsch, Carbon Nanotubes: Basic Concepts and Physical Properties (Wiley-VCH, Berlin, 2004).
[4] G. Zhang, P. Qi, X. Wang, Y. Lu, X. Li, R. Tu, S. Bangsaruntip, D. Mann, L. Zhang, and H. Dai, Science **314**, 974 (2006).
[5] C. M. Yang, K. H. An, J. S. Park, K. A. Park, S. C. Lim, S. H. Cho, Y. S. Lee, W. Park, C. Y. Park, and Y. H. Lee, Phys. Rev. B **73**, 075419 (2006).
[6] Y. Miyata, T. Kawai, Y. Miyamoto, K. Yanagi, Y. Maniwa, and H. Kataura, J. Phys. Chem. C **111**, 9671 (2007).
[7] S. Esconjauregui, B. C. Bayer, M. Fouquet, C. T. Wirth, C. Ducati, S. Hofmann, and J. Robertson, Appl. Phys. Lett. **95**, 173115 (2009).
[8] L. Durrer, J. Greenwald, T. Helbling, M. Muoth, R. Riek, and C. Hierold, Nanotechnology **20**, 355601 (2009).
[9] S. Inoue and Y. Kikuchi, Chem. Phys. Lett. **410**, 209 (2005).
[10] E. W. Wong, M. J. Bronikowski, M. E. Hoenk, R. S. Kowalczyk, and B. D. Hun, Chem. Mater. **17**, 237 (2005).
[11] L. Zhang, Y. Tan, and D. E. Resasco, Chem. Phys. Lett. **422**, 198 (2006).
[12] Y. Murakami, S. Chiashi, Y. Miyauchi, M. Hu, M. Ogura, T. Okubo, and S. Maruyama, Chem. Phys. Lett. **385**, 298 (2004).
[13] S. Maruyama, E. Einarsson, Y. Murakami, and T. Edamura, Chem. Phys. Lett. **403**, 320 (2005).
[14] B. Wang, C. H. P. Poa, L. Wei, L. J. Li, Y. Yang, and Y. Chen, J. Am. Chem. Soc. **9014**, 192 (2007).
[15] X. Li, X. Tu, S. Zaric, K. Welsher, W. S. Seo, W. Zhao, and H. Dai, J. Am. Chem. Soc. **129**, 15770 (2007).
[16] J. Robertson, G. Zhong, H. Telg, C. Thomsen, J. H. Warner, G. A. D. Briggs, U. Dettlaff-Weglikowska, and S. Roth, Appl. Phys. Lett. **93**, 163111 (2008).
[17] H. Telg, J. Maultzsch, S. Reich, F. Hennrich, and C. Thomsen, Phys. Rev. Lett. **93**, 177401 (2004).
[18] V. N. Popov and L. Henrard, Phys. Rev. B **70**, 115407 (2004).
[19] W. H. Chiang and R. M. Sankaran, Nature Mater. **8**, 882 (2009).
[20] S. Hofmann, R. Blume, C. T. Wirth, M. Cantoro, R. Sharma, C. Ducati, M. Hävecker, S. Zafeiratos, P. Schnoerch, A. Oestereich, D. Teschner, M. Albrecht, A. Knop-Gericke, R. Schlögl, and J. Robertson, J. Phys. Chem. C **113**, 1648 (2009).
[21] P. L. Hansen, J. B. Wagner, S. Helveg, J. R. Rostrup-Nielsen, B. S. Clausen, and H. Topsøe, Science **295**, 2053(2002).